

Velocity Distribution in Channels of Rectangular Compound Cross Section

Issam A. AL-KHATIB

*Institute of Community and Public Health,
Birzeit University, West Bank, PALESTINE*

Received 02.12.1996

Abstract

A series of experiments have been carried out in order to measure velocity distribution in a straight symmetrical rectangular compound sections of varying floodplain width, main channel width and step height. Different dimensionless ratios of velocity distributions are obtained and related to relative depth. The geometry effect on the velocity distribution in the main channel and floodplains due to the momentum transfer between the deep section and floodplains has been investigated. The different velocity ratios were generalized and a logarithmic equation for each ratio was determined in such a way that regardless of the model type these equations can be used to calculate velocity ratios within the range of flow conditions examined in this study.

Key Words: Open channel, compound section, velocity distribution.

Dikdörtgen Bileşik Kesitli Kanallarda Hız Dağılımı

Özet

Değişken genişlik ve yüksekliklere sahip düz ve simetrik bileşik dikdörtgen kesitli kanallardan hız dağılımını ölçmek için bir seri deneyler yapılmıştır. Hız dağılımlarının değişik, birimsiz, derinliğe oranlı değerleri elde edilmiştir. Momentum transferinden ötürü anakanal ve tali kanal tabanındaki hız dağılımına kanal geometresinin etkisi incelenmiştir. Değişik hız oranları genelleştirilmiş ve her oran için bir logaritmik bir denklem tanımlanmıştır. Şöyle ki; model tipine bağlı olmaksızın, bu denklemler akış kriterleri çerçevesinde hız oranlarını hesaplamak için kullanılabilirler.

Anahtar Sözcükler: Açık kanal, kompozit kesit, hız dağılımı.

Introduction

A compound channel is characterised by a main channel and at least one floodplain. In dry seasons or in low flows, normally the main channel conveys these flows. Floodplains are used mainly to pass the major flows during the floods.

Owing to simplistic models, calibration with one set of data does not necessarily ensure reliable results

for other data, particularly if for one of the cases the floodplains are inundated. The reduced hydraulic radius of the floodplain and the often higher hydraulic roughness result in lower velocities on the floodplains than in the main channel. These differences referred to as “turbulence phenomenon” (Knight, and Hamid, 1984). There is therefore a lateral transfer

of momentum that results in apparent shear stress.

Because of the difficulty in obtaining sufficient accurate and comprehensive field measurements of velocity and shear stress in compound channels (Bhowmik and Demissie, 1982), considerable reliance must still be placed on well focused laboratory investigations to provide the information concerning the details of the flow structure and the lateral momentum transfer. Such details are important in the application and development of numerical models aimed at solving certain practical open channel flow problems (Brundrett and Baines, 1964).

Several authors have studied compound channels in experiments. In particular, some authors estimate experimentally apparent shear stresses on different possible separation surfaces (Myers, 1978, Wormleaton, et al., 1982, Knight, and Demetriou, 1983), or compare the measured discharges with those calculated on the basis of different subdivisions between main channel and lateral channels (Yen, and Ho, 1983, Knight, et al., 1984, Wormleaton, and Hadjipanous, 1985). Others try to generalize the links between resistance and discharge valid for simple sections (Baird and Ervine, 1984; Myers, 1984; Myers, 1987). Detailed experimental measurements are reported in the aforementioned works and several others (Sellin, 1964; Zheleznyakov, 1966; Rahartnam, and Ahmadi, 1981; Prinos et al., 1985; Lai, 1986; Hollinrake, 1987; Hollinrake, 1988; Lai and Knight, 1988; Hollinrake, 1989; Arnold et al., 1989; Tominaga et al., 1989; Ackers, 1991; Tominaga and Nezu, 1991; Tominaga and Nezu, 1991; Smart, 1992; Rhodes and Knight, 1994).

The aim of this study was to describe the effect of the interaction mechanism on velocity distribution in channel of compound cross section. Specially the effect of the main channel width and step height on the variation of velocity distribution in both main channel and floodplain channel for constant flow discharges investigated.

Theoretical Considerations

To date no theoretical work has been developed for boundary shear and apparent shear due to the momentum transfer from compound channels as a function of relevant quantities. However dimensional analysis may be used to indicate the likely form of that relationship. The method explained by William and Myers (1987) has been followed in this paper.

It may be said that the flow resistance in a

smooth channel forming part of compound section under uniform flow conditions may be expressed as follows:

$$\phi[F, \mu, V_{mc}, V_f, R_{mc}, R_f] = 0 \quad (1)$$

where ϕ = some function of the stated variables; F = boundary shear and momentum shear due to momentum transfer; V_{mc} = average main channel velocity; V_f = average floodplain velocity; ρ = density of fluid; μ = absolute viscosity of fluid; R_{mc} = main channel hydraulic radius; R_f = floodplain hydraulic radius. Since uniform flow has been specified, the weight component in the flow direction is equal and apposite to the shear force, and hence there is no need to include gravitational acceleration.

By a method of dimensional analysis such as the Buckingham π theorem, Eq. 1 may be modified to

$$\frac{F}{\rho V_{mc}^2} = \phi \left[\frac{\mu}{\rho V_{mc} R_{mc}}, \frac{V_f}{V_{mc}}, \frac{R_f}{R_{mc}} \right] \quad (2)$$

Identifying $F/\rho V_{mc}^2$ as a resistance coefficient for the main channel section and combining the last two dimensionless groups yields

$$f_{mc} = \phi \left[(R_e)_{mc}, \frac{(R_e)_{mc}}{(R_e)_f} \right] \quad (3)$$

where $(R_e)_{mc}$ = main channel Reynolds number; $(R_e)_f$ = floodplain Reynolds number. Similar analysis could be presented to show that the resistance coefficients for the floodplain and the full compound cross section are functions of the Reynolds number and Reynolds number ratio. Myers (1984) has presented data to confirm the validity of Eq. 3.

Thus, it is clear that the Reynolds number ratio, $(R_e)_r$, is a significant parameter influencing the flow resistance and hence the carrying capacity of smooth compound channels. Experimental observations, reported later, have concluded that the Reynolds number ratio is independent on channel slope and depends only of channel geometry (Myers, 1987). Thus we may write for a given geometry

$$(R_e)_r = \phi \left[\frac{Y_f}{Y_m} \right] = \phi[Y_r] \quad (4)$$

where $(R_e)_r = (R_e)_{mc}/(R_e)_f$; Y_f = floodplain water depth; Y_m = main channel water depth; Y_r = relative depth which equals the Y_f/Y_m ratio. Hence we may write

$$(R_e)_r = \frac{V_{mc} R_{mc}}{V_f R_f} = \phi[Y_r] \quad (5)$$

and

$$\frac{V_{mc}}{V_f} = V_r = \phi[Y_r] \quad (6)$$

By similar reasoning, it may be argued that the following velocity ratios are also independent of bed slope and depend only on channel geometry

$$\frac{V_{mc}}{V}, \frac{V_f}{V} = \phi[Y_r] \quad (7)$$

Thus, it has been shown that the various velocity ratios defined are functions of channel geometry. These conclusions will be validated and quantified by experimental data.

Experimental Apparatus and Procedure

The experiments were carried out in a glass-walled horizontal laboratory flume 9.0 m long, 0.67 m wide 0.75 m deep, at the Hydromechanics Laboratory of the Middle East Technical University.

Discharge was measured volumetrically with a rectangular sharp crested weir mounted in the inlet box of the flume, Depth measurement over the crest

for this weir was conducted by point gauge reading to the nearest 0.1 mm accuracy and predetermined calibration curve of the weir was used to determine the discharges. The maximum capacity was around 110 lt/sec.

In the course of experiments, for head measurements a point gauge was used along the centreline of the flume. All depth measurements were done with respect to the bottom of the flume. A pitot tube of circular section with external diameter of 7 mm was used to measure the static and total pressures which were used for velocities and shear stresses at required points in the experiments conducted throughout this study.

Models of rectangular compound cross sections were manufactured from Plexiglas and placed at about mid length of the laboratory flume. Fig. 1 shows the plan view, longitudinal profile and cross section of the models with symbols designating important dimensions of model elements. The dimensions of the various models used in the experiments are given in Table 1. In this study model types tested are denoted by BIZJ (I=1, 2, 3; J=1, 2). Here B and Z are the width and step height of the main channel of the compound cross section, respectively.

Table 1. Dimensions and Dimensionless Values of Models

Types of models	B (cm)	Z (cm)	B_f (cm)	BO (cm)	Θ (degree)	β (degree)	BO/ B_f (-)	BO/Z (-)	BO/B (-)	B_f/Z (-)	B_f/B (-)	B/Z (-)
B1Z1	20	5	23.5	67	26.57	153.43	2.85	13.40	3.35	4.70	1.18	4.00
B1Z2	20	10	23.5	67	26.57	153.43	2.85	6.70	3.35	2.35	1.18	2.00
B2Z1	30	5	18.5	67	26.57	153.43	3.62	13.40	2.23	3.70	0.62	6.00
B2Z2	30	10	18.5	67	26.57	153.43	3.62	6.70	2.23	1.85	0.62	3.00
B3Z1	45	5	11.0	67	26.57	153.43	6.09	13.40	1.49	2.20	0.24	9.00
B3Z2	45	10	11.0	67	26.57	153.43	6.09	6.70	1.49	1.10	0.24	4.50

The required experiments first were conducted in the models of smallest B(=20 cm) with varying Z values (=5 cm and 10 cm) and then B was increased to 30 cm at the required amount of Z=5 cm and 10 cm, and finally for B=45 cm with the same two values of Z. The entrance angles, θ and β , were 26.565 and 153.35 degrees respectively. The entrance length, L_e , was twice of the floodplain width, B_f . All the compound cross section models were constructed on a horizontal bottom slope channel.

In order to determine the velocity distribution in the rectangular compound cross sections the channel cross section was divided by a number of successive lines normal to the direction of flow. Then the total and static heads were measured at several points along these normal lines by the use of pitot (Preston) tube. More points were taken close to the channel

boundary. Towards the free surface, the distances between the points where the velocities measured were increased. Figure 2 shows a definition sketch for vertical lines over which velocity measurements were made in models BIZJ, (I=1,2,3 and J=1,2)

Presentation and Discussion of Results

The measured and calculated quantities from the experiments conducted by Al-Khatib (1993) were utilised. In the following sections results of the experiments are summarised.

Velocity distribution patterns were obtained for 11 depths of flow, each corresponding to certain step height only while the others were within the full cross section related to the geometry of each model.

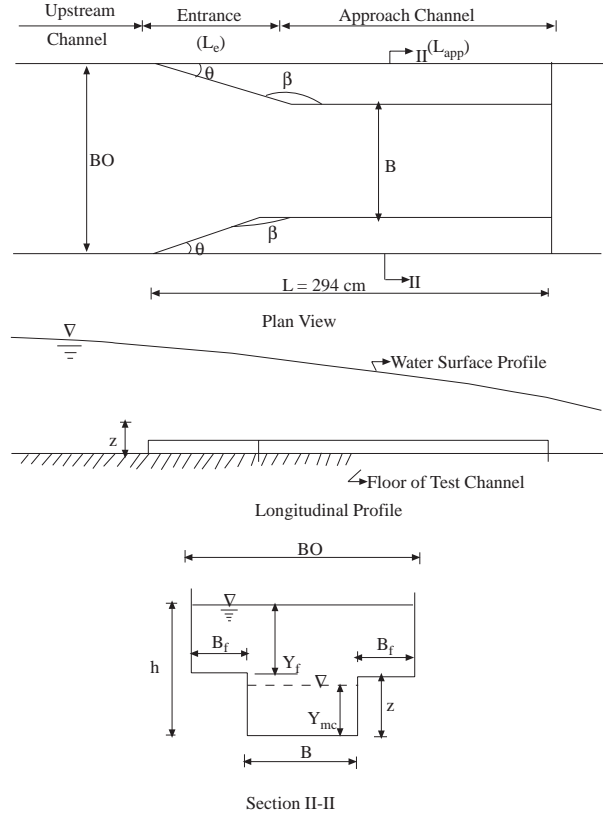


Figure 1. Definition Sketch of the Flume used in the Experiments.

Variation of Reynolds Number Ratio With Relative Depth

In order to see the relationship between the Reynolds number ratio and the relative depth (Eq. 5) Fig. 3 was plotted. From this figure it is clearly seen that for constant step heights, Z , as the main channel bottom width, B , increases, the Reynolds number ratio increases for a given Y_r . Also for constant bottom width, B , as the step height, Z , increases the Reynolds number ratio decreases except models having the largest bottom width, B3Z1 and B3Z2, where the values of the Reynolds number ratio almost coincide with each other. The general trend of the curves given in Fig. 3 show that Reynolds number ratio decreases as the relative depth increases.

Variation of Velocity Ratios V_f/V , V_{mc}/V , V_{mc}/V_f With Relative Depth

Ratios of average main channel velocity and average floodplain velocity to full cross-sectional velocity V_f/V , V_{mc}/V as a function of the relative depth, Y_r are shown in Figs. 4-7 in addition to the curves

obtained from the equation derived by Knight and Demetriou (1983) for V_{mc}/V which will be given later. From these figures it is clearly seen that as the relative depth, Y_r , increases; V_f/V values increase up to a certain value of Y_r and then become almost constant while V_{mc}/V values very slightly decrease. V_{mc}/V ratio is always greater than V_f/V for all the models used in the experiments.

Knight and Demetriou (1983) investigated a smooth symmetrical rectangular compound channel having a bankfull depth of 75 mm, and two floodplains 229 mm wide with a constant bed slop of 0.000966 and a relative depth ranging between 0.1 and 0.5. They presented the following equation for the ratio of main channel to average compound section velocity, V_{mc}/V :

$$\frac{V_{mc}}{V} = 1.0 + 1.08 [(W - 1)Y_r + 1] \left(\frac{W - 1}{W} \right)^{1/4} \times (3.3Y_r)^{4/W} e^{-9.9Y_r} \tag{8}$$

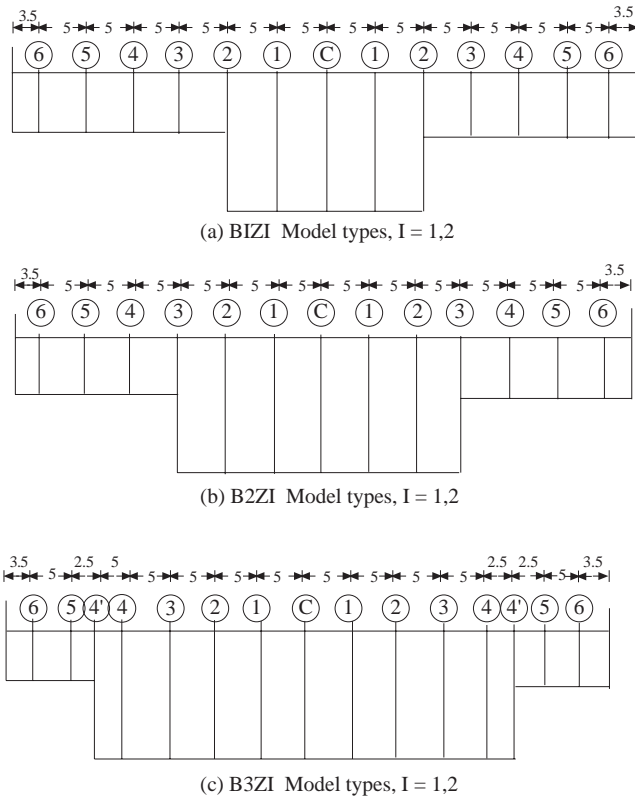


Figure 2. Definition Sketch for Vertical Lines over Which Velocity Measurements were Made for the Different Models, (Dimensions are in cm).

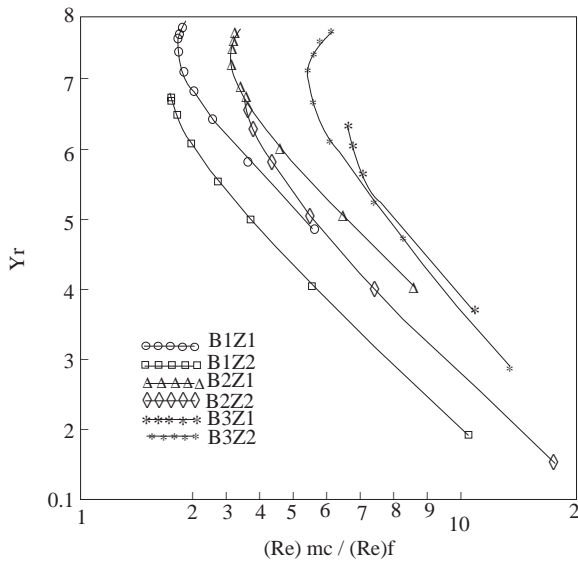


Figure 3. Variation of Reynolds Number Ratio with Relative Depth for Different Models.

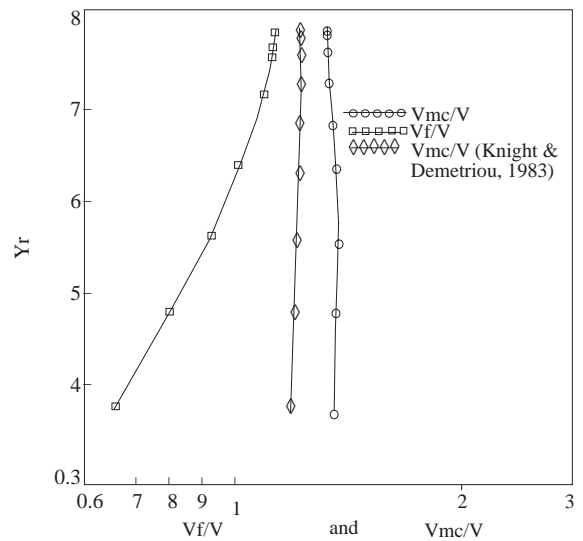


Figure 4. Depth Variation of Ratios of Main Channel and Floodplain to Cross-Sectional Velocities for Model B1Z1.

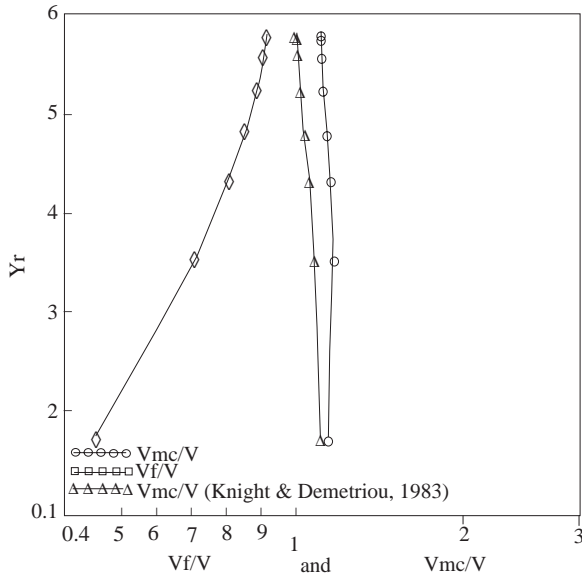


Figure 5. Depth Variation of Ratios of Main Channel and Flooplain to Cross - Sectional Velocities for Model B1Z2.

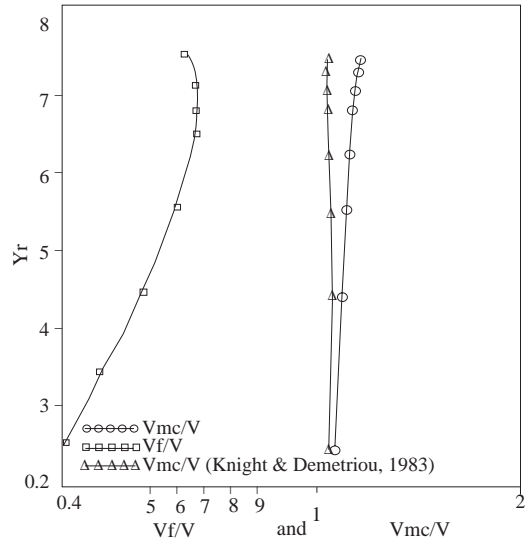


Figure 6. Depth Variation of Ratios of Main Channel and Flooplain to Cross - Sectional Velocities for Model B3Z1.

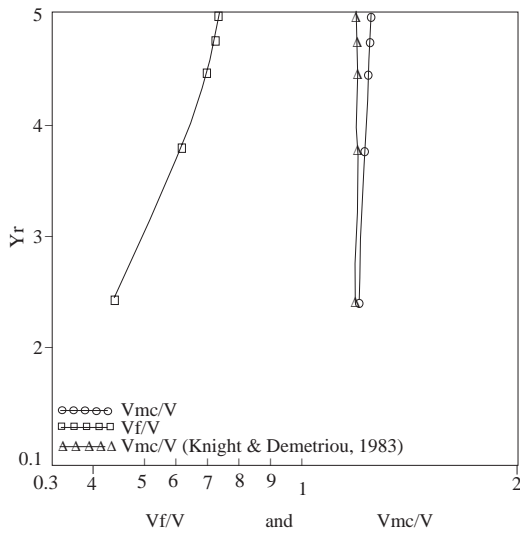


Figure 7. Depth Variation of Ratios of Main Channel and Flooplain to Cross - Sectional Velocities for Model B3Z2.

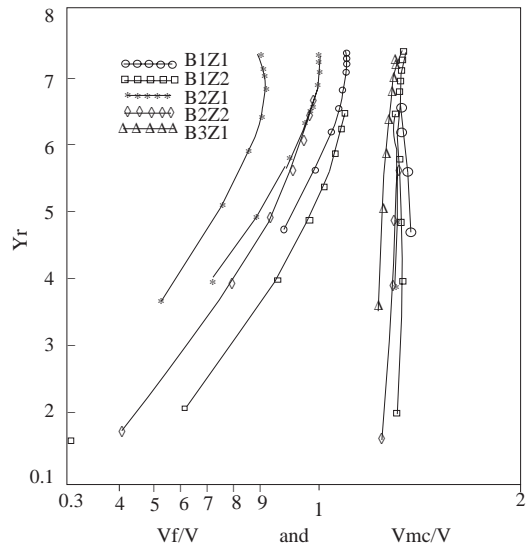


Figure 8. Depth Variation of Ratios of Main Channel and Flooplain to Cross - Sectional Velocities for different Models.

This equation was plotted in Figs. 4-7 to compare the V_{mc}/V ratios given by this equation with those calculated. The analysis of the aforementioned figures shows that Eq. 9 always underestimates the V_{mc}/V ratio and exhibits better results as both main channel width, B , and step height, Z , increase. This is due to the difference in B and Z values in addition

to the bed slope, since the experiments presented in this study were conducted with a horizontal bed channel.

In order to see the effect of main channel bottom width, B , and step height, Z , on the variation of Y_r width V_f/V , V_{mc}/V Figs. 8-10 were plotted. Fig. 8 shows the combination of all the curves given

in Figs.4-7 except those of Knight and Demetriou. Figs. 9 and 10 show the combination of depth variation of ratios of floodplain and main channel to cross-sectional velocities, V_f/V , V_{mc}/V , respectively. From these figures one can say that for a given Y_r the ratio V_f/V , increases as the main channel width, B, decreases. And this ratio also increases as the step height, Z, increases, except those values corresponding to models B3Z2 and B3Z2 where the related curves almost coincide with each other. Also as it was mentioned before V_f/V is a function of Y_r and it is seen that as Y_r values increase the V_f/V ratio increases up to a certain value and then it becomes almost constant. V_f/V values are always less than unity. For Y_r values above 0.6 for model B3ZI I=1, 2) V_f/V values decrease (Figs. 8 and 9) while V_{mc}/V values increase (Figs. 8 and 10). This situation confirms that the momentum transfer is from the floodplain to main channel for Y_r values greater than those mentioned above.

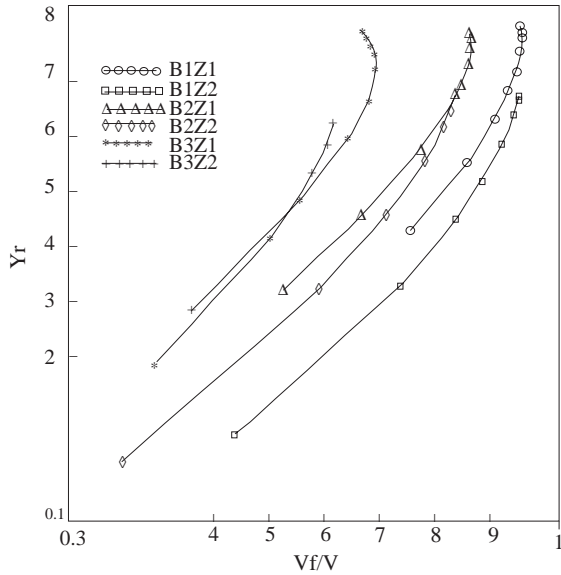


Figure 9. Depth Variation of Ratios of Floodplain to Cross - Sectional Velocities for Different Models.

We had also mentioned that V_{mc}/V ratio was a function of the relative depth, Y_r . So that for a constant Y_r value, the ratio V_{mc}/V increases as the main channel width, B, decreases, and it decreases as the step height, Z, increases. As the main channel width, B, increases V_{mc}/V ratio tends toward unity as seen from the curves of models B3Z1 and B3Z2 which have the largest main channel widths (Fig.10). From

the figure it is also seen that V_{mc}/V is always greater than unity for Y_r values tested.

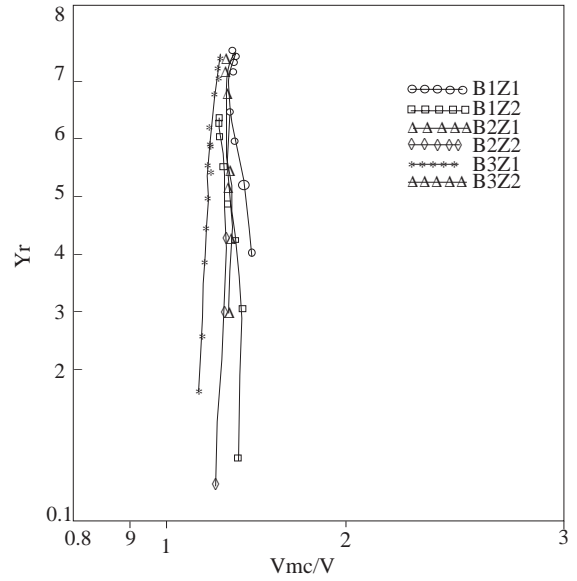


Figure 10. Depth Variation of Ratios of Main Channel to Cross - Sectional Velocities for Different Models.

Ratios of main channel to floodplain velocity, V_{mc}/V_f are shown in Fig. 11 reveals that as the main channel width, B, for the different models, increases, the velocity ratio V_{mc}/V_f increases. The reverse situation occurs as the step height, Z, increase for the same B value while Y_r is kept constant. This is due to having higher rate of increase of V_f/V with increasing Z (Fig. 8) than the rate of decrease of V_{mc}/V with increasing Z (Fig. 10) for a given Y_r value. It can also be seen that the V_{mc}/V ratio is always greater than unity, and tends toward unity for small B values. This result explains the momentum transfer from main channel to floodplains for small floodplain width and the opposite for large floodplain width. In most of the cases, for models of Y_r is about less than 0.7, momentum is transferred from main channel to floodplains.

Regression analysis was used to deduce equations that may be expressed in the general form:

$$\frac{V_{mc}}{V_f} = C(Y_r)^c \quad (9)$$

Table 2 shows the values of C and c obtained for six cross-sections. Also is shown the correlation and average correlation coefficient obtained, which for a line of perfect fit would have a value of ± 1 .

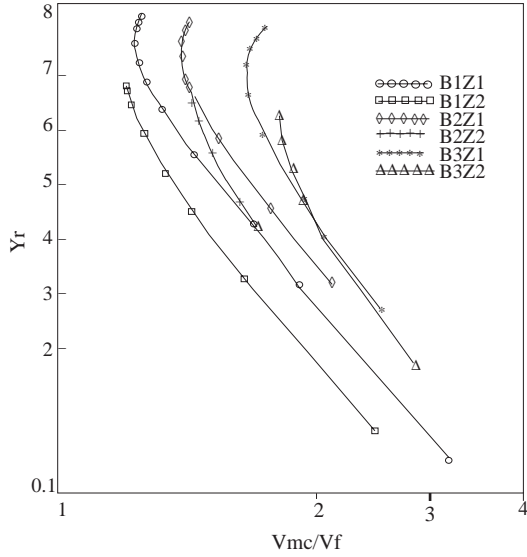


Figure 11. Depth Variation of Velocities Ratio for Different Cross - Sections.

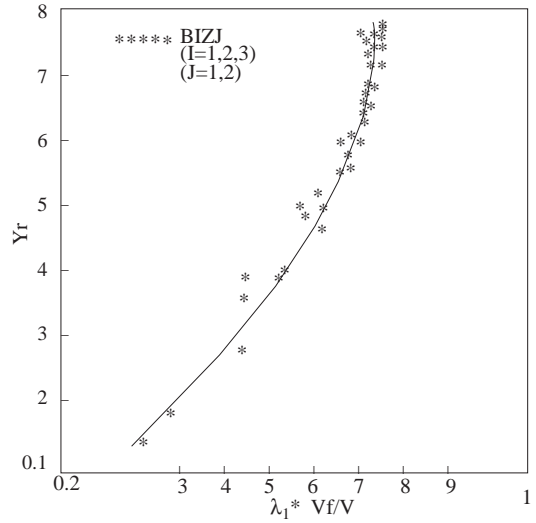


Figure 12. Variation of $\lambda_1(V_f/V)$ with Relative Depth, Y_r , for Models BIZJ (I= 1,2,3; J= 1,2).

Table 2. Values of Exponent, Coefficient and Correlation Coefficient of the Relationship Given by Eq. 9.

Exponent, coefficient and r	Types of models						Average value of r
	B1Z1	B2Z2	B2Z1	B2Z2	B3Z1	B3Z2	
c	-0.374	-0.255	-0.374	-0.483	-0.303	-0.388	
C	1.102	0.884	1.264	1.796	1.549	1.415	
r	0.963	0.993	0.953	0.990	0.912	0.988	0.967

Generalization of the Variation of Velocity Ratios V_f/V , V_{mc}/V , V_{mc}/V_f with Relative Depth

In the previous section it was shown that all of the velocity ratios; V_f/V , V_{mc}/V , and V_{mc}/V_f have different distributions for each model tested as a function of Y_r . However, it is seen that V_f/V versus Y_r , V_{mc}/V_f versus Y_r curves given in Figs. 9-11 for different models, respectively, are almost parallel to each other. From these figures it can also be said that data points of models B3Z1 and B3Z2 almost coincide with each other. This situation may be explained as that for the compound channel of the main channel width B3, the variation of Z does not significantly affect V_f/V , V_{mc}/V , and V_{mc}/V_f values for a given Y_r . For this reason an attempt was made to collect the data of other models on the curves of B3Z2 in each figure (Figs. 9-11). V_f/V , V_{mc}/V , and V_{mc}/V_f vlues of each model given in the aforementioned figures were multiplied by different con-

stants determined in such a way that, best fittings to the curves of model B3Z2 were obtained. These constants of each model, which are called as “shape factors” of the compound cross sections for related velocity ratios are listed in table 3. Since these constants which are designated by λ_i ($i=1, 2, 3$) vary from one model to model, here, they are assumed to be function of B_f/B and B/Z values which describe the geometry of the compound cross sections. Figs. 12-14 show the variation of $\lambda_1(V_f/V)$, $\lambda_2(V_{mc}/V)$ and $\lambda_3(V_{mc}/V_f)$ with Y_r . Except Fig. 14, the others display very good relationship between the related parameters. The equations of the best fitting curves given in these figures are as follows:

$$\frac{V_f}{V} = \frac{\ln Y_r + 3.597}{5.196\lambda_1} \tag{10}$$

$$\frac{V_{mc}}{V} = \frac{\ln Y_r + 8.078}{6.670\lambda_2} \tag{11}$$

$$\frac{V_{mc}}{V_f} = \frac{\ln Y_r - 1.603}{-1.019\lambda_3} \tag{12}$$

Table 3. Values of the Shape Factor, λ_i , ($i=1, 2, 3$)

Types of models	B_f/B	B/Z	Shape factors		
			λ_1	λ_2	λ_3
B1Z1	1.18	4.0	0.674	0.930	1.540
B1Z2	1.18	2.0	0.636	0.930	1.580
B2Z1	0.62	6.0	0.740	0.950	1.320
B2Z2	0.62	3.0	0.760	0.950	1.330
B3Z1	0.24	9.0	0.920	1.000	1.090
B3Z2	0.24	4.5	1.000	1.000	1.000

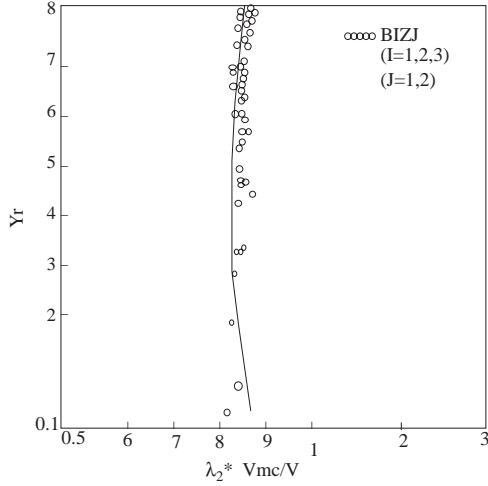


Figure 13. Variation of $\lambda_2(V_{mc}/V)$ with Relative Depth, Y_r , for Models BIZJ ($I= 1,2,3$; $J= 1,2$).

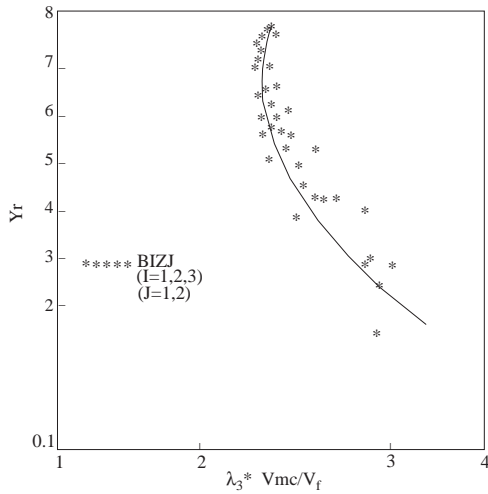


Figure 14. Variation of $\lambda_3(V_{mc}/V_f)$ with Relative Depth, Y_r , for Models BIZJ ($I= 1,2,3$; $J= 1,2$).

Variation of shape factors λ_1 , λ_2 and λ_3 with B_f/B and B/Z are shown in Figs. 15, 16 and 17. As it is seen in each figure there are two curves. These

are upper and lower limit values of B/Z . For a given B_f/B ratio within the range of values tested in this study one can plot a vertical line and intersect the upper and lower limit curves of B/Z . Then applying interpolation for known value of B/Z the value of the shape factor can be obtained from the figure. After that entering the related curve of velocity ratio such as Fig. 12, with the known value of Y_r , $\lambda_1(V_f/V)$, value is read and finally V_f/V ratio can be determined. Applying the above described procedure, for a given value of Y_r of any symmetrical rectangular compound channel which satisfies the B_f/B and B/Z ranges tested in this study, the velocity ratios of V_f/V , V_{mc}/V and V_{mc}/V_f can be estimated.

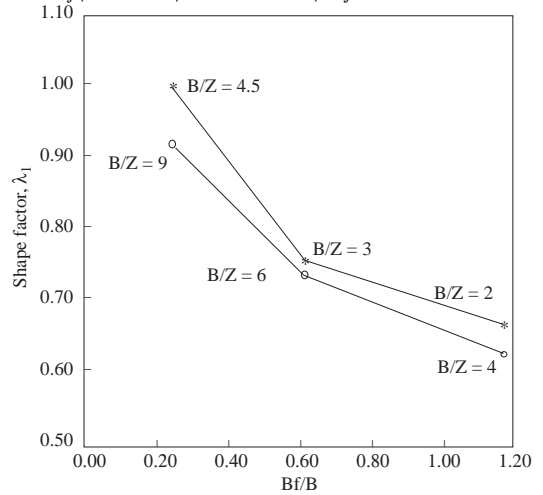


Figure 15. Variation of the Shape Factor, λ_1 , With Floodplain Width to Main Channel Width Ratio.

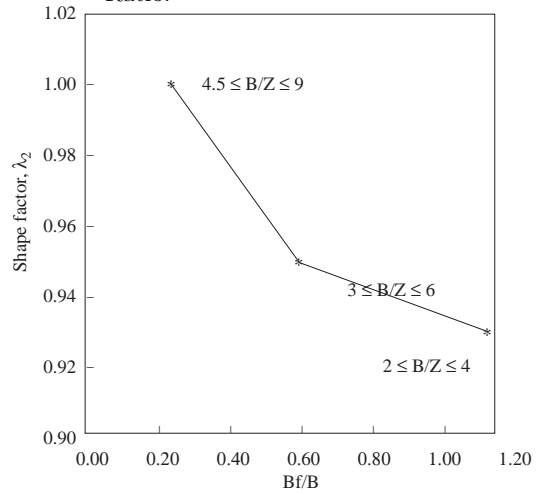


Figure 16. Variation of the Shape Factor, λ_2 , With Floodplain Width to Main Channel Width Ratio.

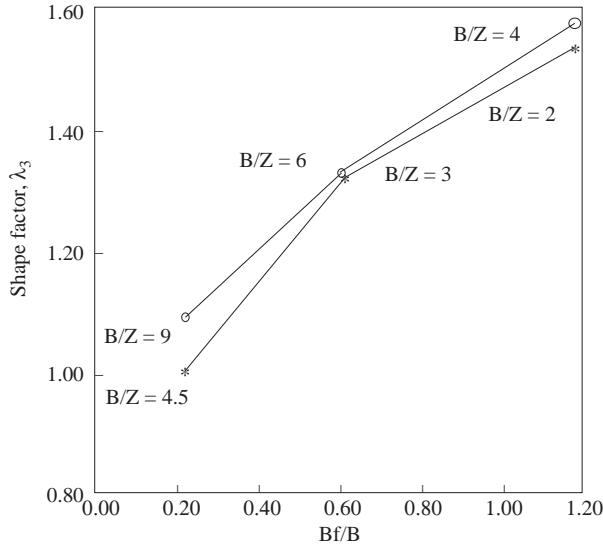


Figure 17. Variation of the Shape Factor, λ_3 , with Floodplain Width to Main Channel Width Ratio.

Conclusions

A series of laboratory experiments has been conducted in a symmetrical rectangular compound cross sectional channel to investigate the geometry effect on the velocity distribution in the main channel and floodplains due to the momentum transfer between the deep section and floodplains has been presented. From the analysis of the experimental results the following conclusions can be drawn:

1. Theoretically it was shown that in symmetrical compound cross sections the resistance coefficient for the main channel, $F/\rho V_{mc}^2$ is a function of $(Re)_{mc}$ and $(Re)_{mc}/(Re)_f$.
2. Reynolds number ratio increases as the value of relative, Y_r , decreases. For a given Y_r , the model having large Z value yields smaller Reynolds number ratio than that of smaller Z value
3. For a given Y_r the ratio V_f/V increases as the main channel width, B , decreases. This ratio increases as the step height, Z , increases.
4. For a constant Y_r value, the ratio V_{mc}/V increase as the main channel width, B , decreases, and it decreases as step height, Z , increases. V_{mc}/V ratio is always greater than unity.
5. The equation of V_{mc}/V (Eq. 9) given by Knight and Demetriou (1983) always under estimates the V_{mc}/V ratio and exhibits better results as both main channel width, B , and step height, Z increases.
6. As the main channel width, B , increases, the velocity ratio V_{mc}/V_f increases. The reverse situation occurs as the setp height, Z , increases for the same B value while Y_r is kept constant. Variation of V_{mc}/V_f with Y_r was expressed by a straight line on a log-log scale (Eq. 10 and Table 2) for each model type.
7. Variation of V_f/V , V_{mc}/V and V_{mc}/V_f were generalized and logarithmic equations for each ratio were determined in such a way that regardless of the model type these equations can be used to calculate velocity ratios within the range of flow conditions examined in this study (Eqs. 11-13).

Notation

The following symbols are used in this paper:

B = bottom width of the approach channel;
 B_f = floodplain channel width;
 BO = bottom width of the upstream channel;
 C, c = coefficient and exponent used in Eq. 10;
 F = boundary shear and momentum shear due to momentum ransfer;
 g = gravitational acceleration;
 L_{app} = approach channel length;
 L_e = entrance channel length;
 Q = volume rate of flow;
 r = correlation coefficient;
 R_f = floodplain hydraulic radius;
 R_{mc} = main channel hydraulic radius;
 $(Re)_f$ = floodplain Reynolds number;
 $(Re)_{mc}$ = main channel Reynolds number;
 $(Re)_r$ = Reynolds number ratio equals to $(Re)_{mc}/(Re)_f$;

V = average full cross-sectional velocity;
 V_f = average floodplain velocity;
 V_{mc} = average main channel velocity;
 Y_f = floodplain water depth;
 Y_{mc} = main channel water depth;
 Y_r = relative depth which equals the Y_f/Y_{mc} ratio;
 Z = step height;
 θ, β = entrance angles.
 λ_i = shape factors for various velocity ratios, $i=1, 2, 3$;
 ϕ = some function of the stated variables;
 ρ = density of fluid;
 μ = absolute viscosity of fluid.

References

- Ackers, P., "Hydraulic design of straight compound channels", Report SR 281, Hydraulics Research, Wallingford, UK, 1991.
- Al-Khatib, I. A. "Hydraulic characteristics and optimum design of symmetrical compound channels for flow measurements", Ph.D. thesis, Middle East Tech. Univ., Ankara, Turkey, 1993.
- Arnold, U. Hottges, J., and Rouve, G., "Turbulence and mixing mechanisms in compound open channel flow", Proc., XXIII IAHR Congr., Ottawa, Canada, A133-A140, 1989.
- Baird, J. I., and Ervine, D. A., "Resistance to flow in channels with overbank floodplain flow", Proceedings of the 1st International Conference on Channels and Channel Control Struct., Springer Verlag, Berlin, Germany, 4.137-4.150, 1984.
- Bhowmik, N. G., and Demissie, M., "Carrying capacity of floodplains", J. Hydr. Engrg., ASCE, 108, No. HY3, 443-452, 1982.
- Brundrett, E., and Baines, W. D., "Production and diffusion of vorticity in duct flow", J. Fluid Mech., 19(3): 375-394, 1964.
- Hollinrake, P.G., "The structure of flow in open channels-a literature search", Report SR 96, Hydraulics Research, Wallingford, UK, 1987.
- Hollinrake, P. G., "The structure of flow in open channels-a literature search", Vol. 2 Report SR 153, Hydraulics Research, Wallingford, UK, 1988.
- Hollinrake, P. G., "The structure of flow in open channels-a literature search", Vol. 3 Report SR 209, Hydraulics Research, Wallingford, UK, 1989.
- Myers, W. R. C., "Momentum transfer in a compound channel", J. Hydr. Research, 16(2): 139-150, 1978.
- Knight, D. W., and Demetriou, J. D., "Flood plain and main channel flow interaction", J. Hydr. Engrg., ASCE, 109(8), 1073-1092, 1983.
- Knight, D. W., Demetriou, J. D., and Hamid, M. E., "Stage discharge relationships for compound channels", Proc., 1st Int. Conf. on channels and channel control struct., Springer Verlag, Berlin, Germany, 4.21-4.25, 1984.
- Knight, D. W., and Hamid, M. E., "Boundary shear in symmetrical compound channels". J. Hydr. Engrg., ASCE, 109 (10): 1412-1427, 1984.
- Lai, C. J. "Flow resistance, discharge capacity and momentum transfer in smooth compound closed ducts", Ph.D. Thesis, University of Birmingham, U. K, 1986.
- Lai C. J., and Knight, D. W., "Distributions of streamwise velocity and boundary shear stress in compound ducts". Proc. 3rd Int. Symp. on Refined Flow Modelling and Turbulence Measurements, IAHR, Ed. Iwasa, Y., Tamai, N. and Wada, A., Tokyo, Japan, 1988.
- Myers, W. R. C., "Momentum transfer in a compound channel", J. Hydr. Research, 16(2): 139-150, 1978.
- Myers, W. R. C., "Frictional resistance in channel with flood plains", Proceedings of the 1st International Conference on Channels and Channel Control Struct., Springer Verlag, Berlin, Germany, 4.73-4.87, 1984.
- Myers, W. R. C., "Velocity and discharge in compound channels" J. Hydr. Engrg., ASCE, 113(6): 753-766, 1987.
- Prinos, P., Townsend, R., and Tavoularis, S., "Structure of turbulence in compound channel flows", J. Hydr. Engrg., ASCE, 111(9): 1246-1261, 1985.
- Rahartnam, N., and Ahmaid, R., "Hydraulics of channel with flood-plains", J. Hydr. Res., 19(1), 43-60, 1981.
- Rhodes, D. G., and Knight, D. W., "Velocity and boundary shear in a wide compound duct", J. Hydr. Research, ASCE, 32(5): 743-764, 1994.
- Sellin, R. H. J., "A laboratory investigation into the interaction between the flow into the channel of a river and that over its flood plain", Houille Blanche, 19(7): 793-802, 1964.
- Smart, G. M., "Stage-discharge discontinuity in composite flood channels", J. Hydr. Res., 30(6): 818-833, 1992.
- Tominaga, A., Nezu, I., "Turbulent structure in compound open channel flow", J. Hydr. Engrg., ASCE, 117(1): 21-41, 1991.
- Tominaga, A., Nezu, I., and Ezaki, K., "Experimental study on secondary currents in compound open-channel flow", Proc., XXIII IAHR Congr., Ottawa, Canada, A15-A22, 1989.
- Wormleaton, P. R., Allen, J. and Hadjipanous, P., "Discharge assessment in compound channel flow", J. Hydr. Div., ASCE, 108(9): 975-994, 1982.
- Wormleaton, P. R., and Hadjipanous, P., "Flow distribution in compound channels", J. Hydr. Engrg., ASCE, 111(2): 357-361, 1985.
- Yen, C. L., and Ho, S. Y., "Discussion of discharge assessment in compound channel flow", by P. R. Wormleaton, J. Allen and P. Hadjipanous, J. Hydr. Engrg., ASCE, 109(11): 1561-1567, 1983.
- Zheleznyakov, G. V., "Relative deficit of mean velocity of unstable river flow, kinematic effect in river beds with flood plains", Proc. 11th IAHR Congress, 1966.